International Journal of Recent Technology and Engineering (IJRTE)
ISSN: 2277-3878, Volume-8 Issue-4, November 2019

An Access for Designing and Manufacturing of Aerodynamics Wings for a FSAE Vehicle

Anirudh Ganesh Sriraam, Sangeet Aggarwal, Savitoj Singh Aulakh, Jamadagni Nagesh Adarsh , Shaswat Kumar Singh

Abstract— An Airfoil has various parameters, controlling which, it is possible to design an application specific shape to serve a certain purpose. These parameters include, but are not limited to, Chord, Camber, Maximum Camber Position, Thickness, Maximum Thickness Position, Leading Edge Radius and Trailing Edge Radius. This research seeks to study the effect of change in such parameters in the design of a Custom Airfoil, for the application in the Front Wing of Formula Student Car. With most Formula Student Cars being traction limited, high-lift low aspect-ratio wings are desired for optimal increase in Lateral Acceleration under cornering circumstances. Owing to the relatively softly sprung nature of the car, it is also desirable to have a wing which is less sensitive to changes in ground proximity. Taking these factors into consideration, this paper delves into the design of a Custom Airfoil by varying four major parameters- Camber, Maximum Camber Position, Thickness, Maximum Thickness Position. The research then proceeds to manufacture the complex shape in the most economically efficient manner.

Keywords : Airfoil Parameterization, Wet layup, Composite Material, Computation Two Dimensional Simulation

I. INTRODUCTION

The Implementation 0020 of Airfoil Wings was first seen in 1967 on the LOTUS 49 Formula One Car. The inverted Wings would provide negative lift which in turn would increase the normal load on the tires, increasing the available grip. This philosophy took off quite early, and the aerodynamic development has seen exponential growth, limited not only to motorsports but, in the Automotive Sector as well.The same philosophy found its way into formula student as well. With the rules being relatively lenient, teams were found to gain a considerable advantage by using wings, owing to which the rules were subsequently made more stringent. This has resulted in the heightened importance of a high lift low aspect ratio wing to cope with the Formula Student tracks with a majority of slow corners. The front wing is aerodynamically more efficient in comparison to the rear wing, owing to its close proximity to the ground and hence working under 'Ground Effects'. As a result, the front wing is sensitive to variation in Ride-Height. A change in ride height is inevitable under cornering conditions as a result of which variations in downforce is observed during the same. A number of experiments were
conducted for an inverted wing in ground effects previously [9-12] .

Now with the growing competition in formula student teams it is hard to invest weight in non-structural components thus arrives to motive to make the structures as light as possible[5]. It is equally important to make the structures reasonably stiff to prevent any atonement of aerodynamic effect. The aforementioned properties and material requirements are very unlikely to be fulfilled by any other class of materials except composites[1]. Emergence of reinforcements like carbon fiber [2] and matrix like epoxy has assisted in meeting the complex requirements by the virtue of their high performance in the proven standards of the strength to weight ratio.

The manufacturing aspect of these advanced composites is equally important as the properties are not only affected by the type of reinforcement and matrix but also the composition in which they are important. The work describes a manufacturing method for a low density sandwich-core laminate composite aerofoil[4], more particularly, that cut downs manufacturing cost, enhances structural strength, augments structural integrity and reduces overall structural weight[3]. Thus, a goal-oriented approach of selection of material along with a detailed course of manufacturing process is presented while reiterating the project integration with complete vehicle parameters[6].

The effect of ground proximity has been previously studied by Zerihan and Zhang [9]. The results revealed an initial increase in downforce followed a sudden reduction in the same, when the wing is placed at a height lower than the height at which maximum downforce was being achieved. The height that was finalized as per them was 50mm. Beyond this point the airfoil began to lose its downforce. Flow Separation is a result of the presence of an adverse pressure gradient where the flow separates from the surface as the momentum is reduced. Separation near the trailing is observed at moderate Ride Heights.

Manuscript published on November 30, 2019.
* Correspondence Author
Shaswat Kumar Singh*, Anirudh Ganesh Sriraam, VIT Vellore, Tamilnadu, India Manav Badamwala, Student, VIT Vellore, Tamilnadu , India
Sangeet Aggarwal, VIT Vellore, Tamilnadu , India Manav Badamwala, Student, VIT Vellore, Tamilnadu , India Savitoj Singh Aulakh, VIT Vellore, Tamilnadu, India Manav Badamwala, Student, VIT Vellore, Tamilnadu , India
Jamadagni Nagesh Adarsh, VIT Vellore, Tamilnadu, India Manav Badamwala, Student, VIT Vellore, Tamilnadu , India
Shaswat Kumar Singh, VIT Vellore, Tamilnadu, India Manav Badamwala, Student, VIT Vellore, Tamilnadu , India

However, as the proximity to the ground increases, the region of separated flow increases resulting in loss of performance. Studies by Zerihan and Zhang stated that the momentum of the air when separated slowed down [5,6].

The edge vortices reduced the wings performance and were studied extensively by Zerihan and Zhang [12]. Hence the downforce needed to be sufficient enough to provide performance benefits and also lose a certain bit in this interaction.

Airfoils have various parameters, which can be changed according the required application and functional needs. This paper investigates the development of a customized Airofoil for specific application in the front wing of a formula student car, while addressing the need for high lift and reduced sensitivity to ground proximity. The primary objective was to develop an efficient multi-element wing system with minimized sensitivity to ground proximity and high lift.

II. METHODOLOGY

1. Aerodynamics Package Design

The Front-Wing design starts off with the 2-D selection, design and optimization of Airfoils. The Reynolds Number Range is first chosen according the length of the car and the flow velocity. The Reynolds Number is the ratio of the inertial forces to the viscous forces. It is a dimensionless number which describes the nature of the flow, which can namely be of two types. It can be a viscous dominated flow in which case it would be 'laminar' or it can be eddy dominated which would make it turbulent. The Reynolds number is given by:

$$Re = \frac{\rho v l}{\mu} = \frac{v l}{\vartheta}$$

Where,

v = *Velocity of the fluid*
l= *The characteristic length (Chord Width)*
ρ = *The density of the fluid*
μ =*The dynamic viscosity of the fluid*
υ = *The kinematic Viscosity of the fluid*

The characteristic length is chosen to be between 400mm and 700mm The flow velocity was set at 10 m/s, which was the average cornering velocity of the FSAE car in question on an Autocross track, obtained from the Data Acquisition Sub-System. This translated to a Reynolds number between 200,000 and 500,000.

a. Velocity Selection

The velocity chosen for CFD simulation was 10 m/s by undertaking the following procedure.

The driver was asked to do multiple laps at his full potential on a track that was set up according to the Skid Pad track specifications as specified in the FSAE 2019 rulebook. The Speed data from an autocross lap was logged using the in built GPS of the data logger (Fig 1). The data was filtered twice, followed by removing any offset that was present. This was followed by performing the concerned unit conversions to obtain the data in m/s.

Fig. 1: Velocity Logged By the GPS and histogram

Next, a histogram was plotted with proportion percentage on the Y axis and the speed data in m/s to find out the most frequently occurring speed value. Further, the average velocity of the whole lap was then also calculated to better support and justify the histogram data. This analysis helped to choose the simulation speed as 10 m/s.

b. Airfoil selection

The airfoils were selected from an online airfoil database amongst various low Reynolds Number - high lift foils. During the shortlisting process, airfoils with high Cl values at relatively lower angles were targeted. In addition, airfoils with abrupt changes in lift were avoided while high Cd values at low angles were avoided as well. The Airfoils that were shortlisted were: Selig 1223, CH-10-48-13, AH-79-100C, EPPLER 420, FX 74-C15 MOD (Fig 2).

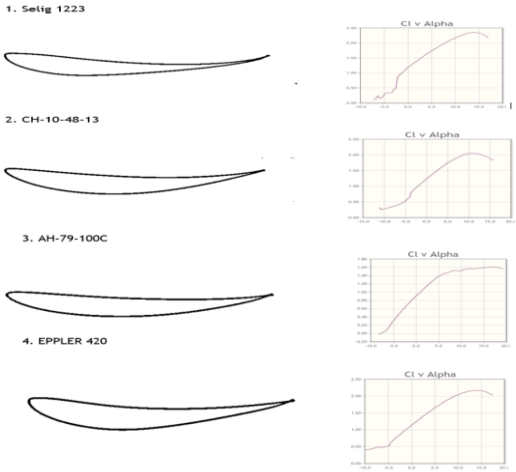

Fig. 2: Shortlisted Airfoils

All the five shortlisted airfoil possessed high Cl values. The AH-79 showed a very flat curve near the peak Cl which was desirable, however the high Cl values possessed by the Selig 1223 was more desirable for the baseline airfoil as it would further modified to tackle the pitch sensitivity.

c. Airfoil Modification

The primary objective was to design a front wing with reduced pitch sensitivity. This could be achieved by modifying the base airfoil to acquire the desired characteristics. This process was carried out through XFLR – 5 and StarCCM+. XFLR-5 is an airfoil design and analysis software which can be used to change various parameters of an airfoil. The parameters that were modified were: Camber, Maximum Camber Position, Thickness, Maximum Thickness Position.

There parameters were first varied in XFLR5, following which the 2-D shape was imported into SolidWorks. After creating a Parasolid it is then imported onto StarCCM+ to carry out the 2-D simulations. This process was repeated till a combination of all the parameters are obtained. It was observed that the camber had the highest bearing on the performance of the Airfoil followed by the Maximum Camber Position, Thickness and Maximum Thickness Position.Fig 3 shows the difference in the final optimized profile and initial selig s1223.

The effects of the camber position and camber thickness can be seen in fig 5. This gives the inference that there is a pattern observable and optimized profile was later found for rest of the profiles.

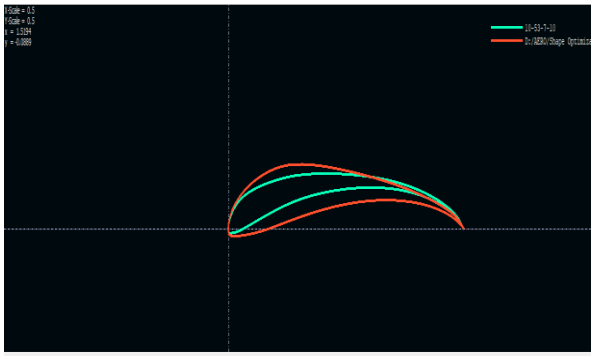

Fig. 3: New(green) vs Old(red) airfoil

Through optimization using XFLR5 and StarCCM+ the downforce was increased by 60%, while the downforce loss under pitching condition was reduced to 5% from 25%

d. Simulation Set-up

The simulations were confined to 2 Dimensions and steady state owing to the high convergence rates. 2-Dimensional Models are best suited for analysis of Airfoil shapes. Simulations were carried out on StarCCM+, which is a Multiphysics CFD software. The mesh cell count was 140,000 Cells.

The Polyhedral mesh was selected with the prism layer mesher (fig 6) for meshing the subtracted tunnel. The polyhedral mesh is capable of accommodating complex curvatures, which would ensure that the Airfoil shapes are accurately meshed. The prism layer mesh is used to capture the boundary layer while targeting a y+ of greater than 30.

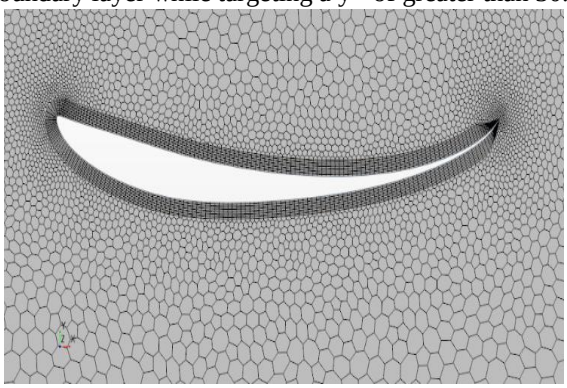

Fig. 6: Effect of Camber and Max. Camber Position variation

SST Menter K-omega model was used to model the turbulence. The SST Menter K-omega model excels at modelling near wall flows using the k-omega equations and it models the far-field flows using the k-epsilon model. The k-omega model is usually used to monitor near wall flows as it excels in predicting separation, while the k-epsilon model is suitable for far field flows and takes up less resources. The SST Menter K-Omega Model ensures that the best of both worlds are incorporated into one single model. The table 1 shows the physics models employed for the simulation of airfoil.

The fig 7 and fig 8 show the difference the optimization of parameters such as camber thickness and camber position effect the downforce and drag values.

The final simulations were checked for mesh independency and the error percentage was only up to 2.3%. The pressure distribution was the scalar quantity measured for the post processing.

An automated code was created to automate the setup and saving the images for post processing. The code was done via JAVA language and the macro functionality of the software was used to process batches of airfoils. This saved time and provided a huge database to work with.

Table 1: Simulation Models

PHYSICS CONTINUUM
MODELS
All y+ Wall Treatment
Exact Wall Distance
SST (Menter) K-Omega
Reynolds-Averaged Navier Stokes
Constant Density
Gradients
Segregated Flow
Gas
Steady
Two Dimensional

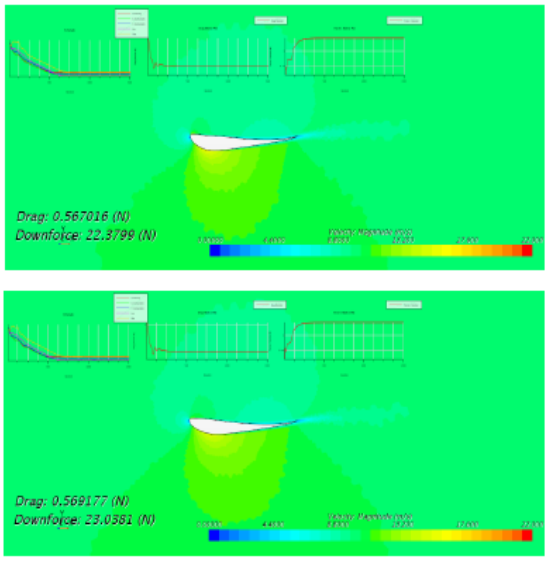

Fig. 7: Effect of Camber and Max. Camber Position variation (Initial and Final Iteration)

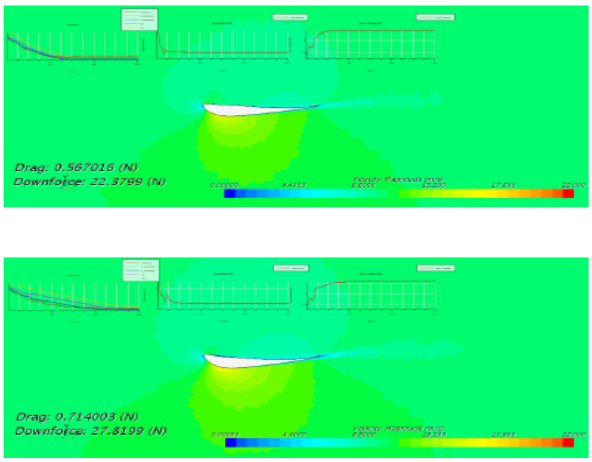

Fig. 8: Effect of Camber and Max. Camber Position variation (Initial and Final Iteration)

Table 2: Simulation Iterations

Cam.	Cam. Pos	Scalar	Downforce	Drag
5	50	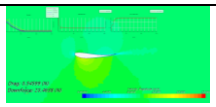	020.46	0.54
6	50	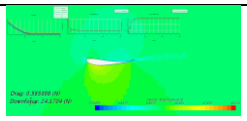	24.17	0.58
7	50	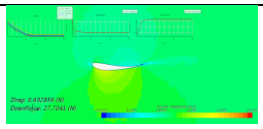	27.7	0.63
8	50	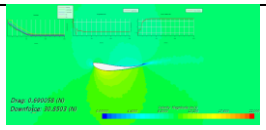	30.85	0.69
9	50	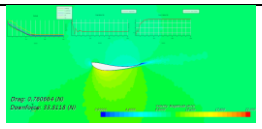	33.81	0.76
10	50	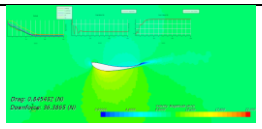	36.38	0.84
5	60	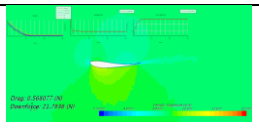	21.76	0.56
6	60	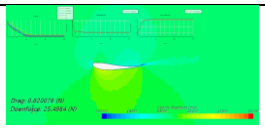	25.49	0.62
7	60	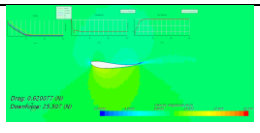	25.5	0.62

The table 1 shows the various iteration conducted for the camber and camber position optimization. The Front Wing was chosen to have a multi element design to promote pressure recovery and hence increase the downforce that can be obtained from the Main Element. Before proceeding to the 3-D multi-element simulations, 2-D simulations were carried out to set the position and the angle of various flaps.

The Airfoil for the flap was selected to be the same Airfoil as the main element, owing to its forward Maximum Camber position, thin section and high downforce yields. The flaps in a multi element system are usually used primarily for pressure recovery and don't generate a high amount of downforce themselves. However, by using the modified airfoil, the flaps not only aided in pressure recovery, but also generated a considerable amount of downforce themselves.

Owing to the formula student rule constraints, which doesn't allow Aerodynamic elements in front of the front tire to be more than 250mm, a single flap was used in front of the front tire and two flaps were used on the inner section. Pressure recovery was achieved on the both the inner and outer sections through an iterative process. A gurney flap was used on the outer section to promote vortex shedding and hence flow attachment with only one flap present.

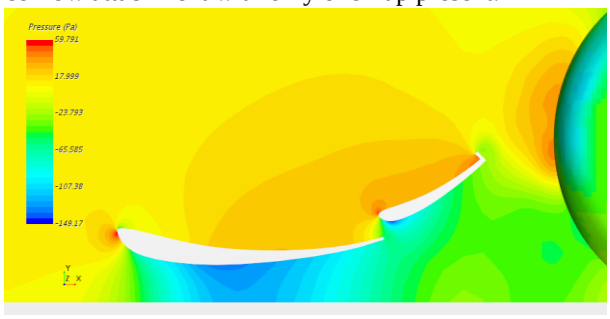

(a)

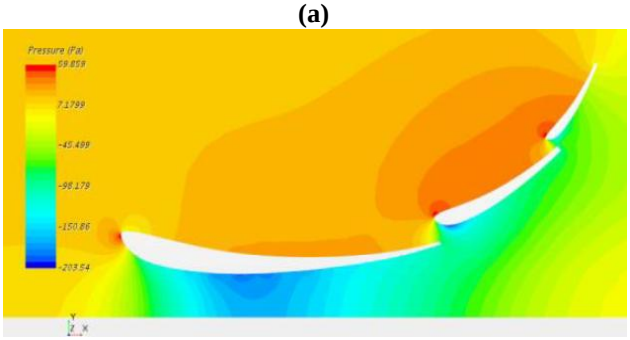

(b)

Fig. 9: (a)Outer Section of the wing (b) Inner Section of the Wing

Table 2: Final Optimized Angles

Element Type	Angle in Degrees
Main Element	3.5
1st Flap	34
2nd Flap	60

The final H/C ratio was chosen to be 0.154, the Chord length of the main element was chosen to be 421mm and the final wing height was chosen to be 65mm.

e. 3-D Optimization

Although 2-D simulations are fast and robust, they fail to take into account many three dimensional occurrences, namely the formation of wing tip vortices. The Endplate is used in the front wing to maintain the pressure differential above and below the wing. The size of the endplate in constrained by the following according to the formula student rules: The height is to be less than 250mm, the furthest point from the front of front wheel to be less than 700mm, the height from the ground to be more than 30mm and the aft most section of the endplate must be at least 75mm from the front of the front tire. Keeping the above constraints in mind, the endplate was first made to intersect with the floor of the tunnel and the bottom section of the endplate was raised in an iterative process to obtain least endplate size while ensuring the pressure differential is being maintained(fig 10). A similar process was followed for the inner endplates as well.

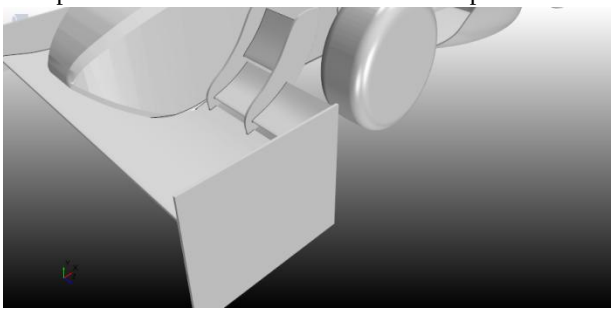

Fig. 10: Initial Iteration for endplate Optimization with large endplates

The next step was to further seal the flow on the underside of the wing. A common way of achieving this is to use a device known as a 'footplate' which captures the incoming airflow to create and house a strong vortex, hence ensuring the underside of the wing is effectively sealed. The Footplate was designed to ensure that a strong vortex is created which is sustained through the length of the endplate. The iterations began is a diameter of 12 mm, due to the limitation of manufacturing. The diameter was gradually increased to optimize the optimal diameter. The optimal diameter was found to be 36 mm at 10m/s (Average cornering velocity) and 40mm at 14 m/s (vehicle's average speed in a endurance track) . The combination of both with the diameter increase along the axis of vehicle from 30mm to 40mm and decreasing from 40mm to 30mm where iterated. The final optimized the footplate that was chosen was the 36 mm diameter footplate as it performed the best in cornering situations.

The simulation used a quarter body for the reducing the simulation burden and faster results (As shown in fig 11). The mesher model used for footplates was a polyhedral mesh also. The mesh cell count was 5,884,923.The choice of polyhedral was done for maintaining accuracy of the simulation and capturing the curvature of such a small device. This can be seem in fig 12.

The footplate were decided to be a part of the final wing assembly due to its ability to increase the aspect ratio in a confined space. The gurney flap was later decided to be incorporated in the airfoil trailing edges for vortex shedding phenomenon to occur and enable the wing to be kept at higher degrees of attack.

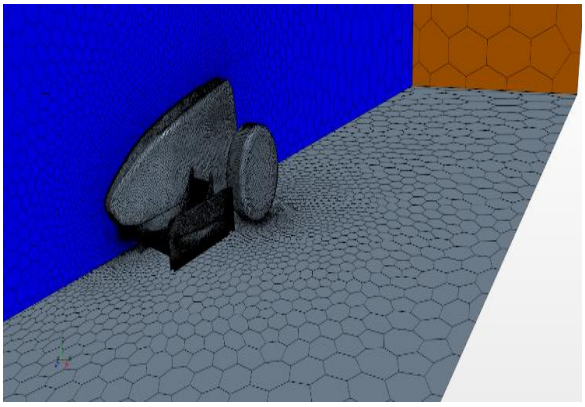

Fig. 11: Quarter Body Mesh

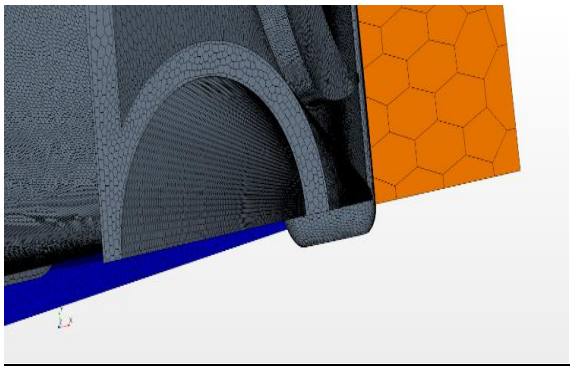

Fig. 12: Footplate Curvature Coverage

To ensure that the vortex is sustained through the length of the endplate, a gurney flap was introduced at the end of the endplate. The models incorporated for the simulation were similar to 2 Dimensional simulations except this time the simulations were conducted in 3 dimensional space. The gurney flap would aid in vortex shedding, creating an acute low pressure region right behind the footplate exit, hence creating a strong suction effect for the vortex. In addition, the low pressure created by the gurney and the vortex help reduce the recirculation zone right in front of the front tire, which has a negative effect on the performance of the front wing. The length of the gurney was fixed at 36mm to entirely cover the footplate for manufacturing ease. Table 4 shows all the iteration conducted. The Graph shows that majority of the increase was seen after the diameter was increased to 36mm. Later only a difference of 2N downforce was seen (fig 14). This was negligible and 36mm design was adopted.

Fig 14 and fig 16 show the vortex being formed under the wing effectively sanctioning the air and creating a barrier. The resampled volume was created for the pressure scalar and was found to have reduced the high pressure recirculation zone in front of the tire(fig 15).

The final designed model was taking through mesh independency and an error percentage of 3.2 % was observed. Making the simulation mesh independent and accurate.

The curved footplates where not iterated due to restrictions due to space and unnecessary complexity.

Table 3: Simulation Models

PHYSICS CONTINUUM
MODELS
All y+ Wall Treatment
Exact Wall Distance
SST (Menter) K-Omega
Reynolds-Averaged Navier Stokes
Constant Density
Gradients
Segregated Flow
Gas
Steady
Three Dimensional

Table 4: Footplate Simulation Data

Name	Downforce	Drag
Normal	85	14
Diameter-12mm	87.2	14.3
Diameter-24mm	91.9	14.2
Diameter-36mm	98.6	14.3
Diameter-44mm	95.25	14.3
Diameter-40mm	98.8	14.75
Incremental Diameter-30mm-40mm	96.2	14.6
Decremental Diameter-40mm-30mm	96.15	14.6

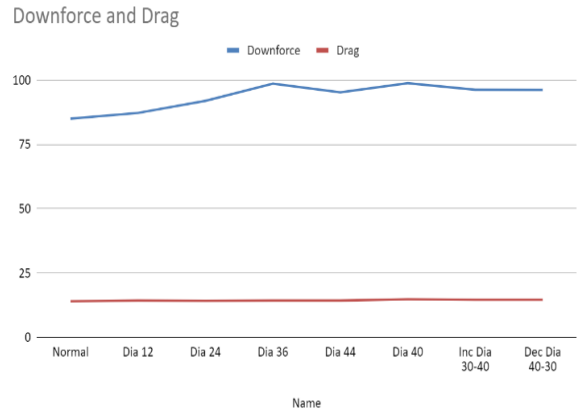

Fig. 13: Graph for increase in downforce due to footplate

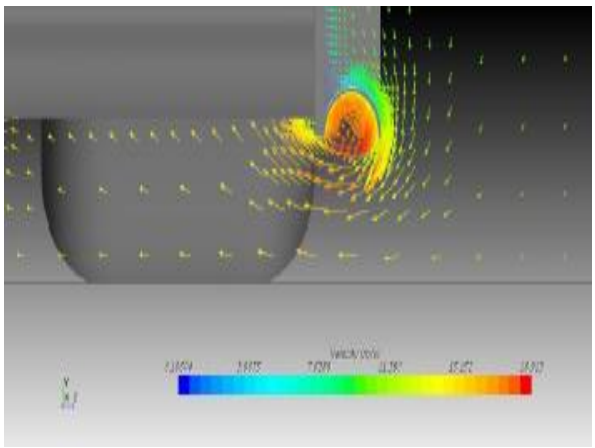

Fig. 14: Vector Scene showing the formation of vortices

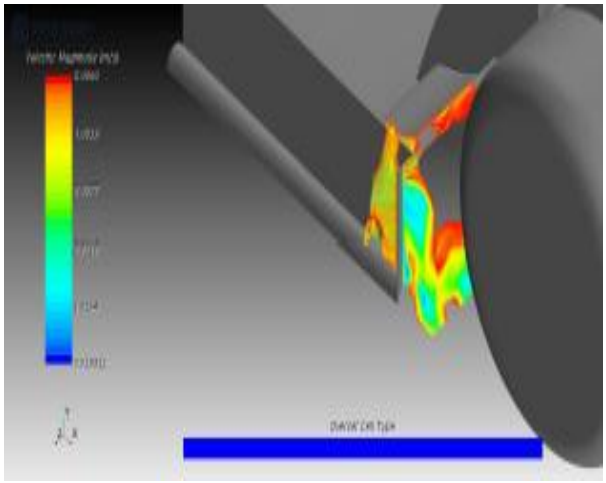

Fig. 10: Resampled Volume showing the reduction in the recirculation zone

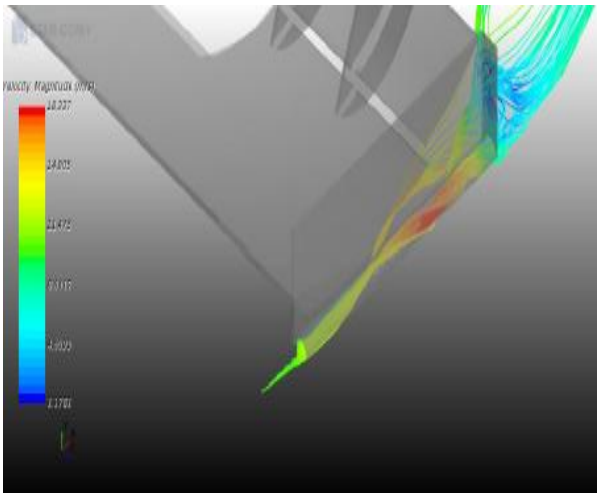

Fig. 16: Streamlines showing the formation of vortex and shedding behind the gurney

f. Results

The airfoil was first selected based on the flow velocity and hence the Reynolds Number. Following this, XFLR-5 was used to modify the shape of the airfoil to ensure high lift at low speeds coupled with reduced pitch sensitivity. Following the modification to the standard S-1223.

Among the four parameters which were varied, it was found that camber seemed to have the highest weightage on the performance of the airfoil. Varying the camber on XFLR-5 while keeping all the other values constant, gave a rise to as much as 2-3 N of downforce variation per camber iteration. Following this, the camber position played a major role in ensuring optimum downforce as it had a direct bearing on the areas of favorable and unfavorable pressure gradients. Following these two parameters, the thickness and thickness position variation play the role of fine tuning the efficiency of the airfoil by bringing about minute changes in is frontal area.

Table 5: Final Results

Cam	Cam Pos.	Thickness	Thickness Pos.	Downforce (N)	Drag (N)
5	30	5(O)	20(O)	24.646	1.189
6	30	5(O)	20(O)	22.379	0.567
7	30	5(O)	20(O)	25.43	0.61
8	30	5(O)	20(O)	27.819	0.714
9	30	5(O)	20(O)	29.151	0.937
10	30	5(O)	20(O)	31.147	0.989
5	40	5(O)	20(O)	19.324	0.534
6	40	5(O)	20(O)	23.0381	0.569
7	40	5(O)	20(O)	26.536	0.609
8	40	5(O)	20(O)	29.7424	0.658
9	40	5(O)	20(O)	32.799	0.721
10	40	5(O)	20(O)	35.18	0.807
5	50	5(O)	20(O)	20.4638	0.545
6	50	5(O)	20(O)	24.17	0.585
7	50	5(O)	20(O)	27.704	0.632
8	50	5(O)	20(O)	30.85	0.69
9	50	5(O)	20(O)	33.8118	0.76
10	50	5(O)	20(O)	36.386	0.845
5	60	5(O)	20(O)	21.763	0.568
6	60	5(O)	20(O)	25.498	0.62
7	60	5(O)	20(O)	25.507	0.62
8	60	5(O)	20(O)	25.458	0.62
9	60	5(O)	20(O)	34.29	0.869
10	60	5(O)	20(O)	36.284	0.992
10	53	1	10	37.399	0.829
10	53	2	10	37.121	0.831
10	53	3	10	36.742	0.84
10	53	4	10	36.649	0.848
10	53	5	10	36.619	0.857
10	53	6	10	36.504	0.859
10	53	7	10	35.65	0.888
10	53	1	20	36.728	0.836
10	53	2	20	36.492	0.844
10	53	3	20	36.635	0.846
10	53	4	20	37.298	0.859
10	53	5	20	36.584	0.86
10	53	6	20	36.386	0.877
10	53	7	20	36.343	0.889
10	53	1	30	35.959	0.868
10	53	2	30	36.328	0.862
10	53	3	30	36.433	0.864
10	53	4	30	36.466	0.871
10	53	5	30	36.374	0.889
10	53	6	30	35.947	0.893
10	53	7	30	35.92	0.908

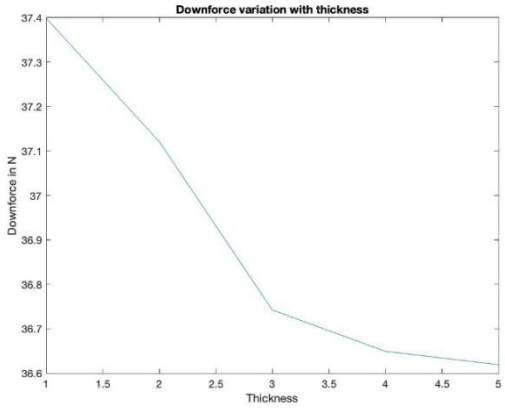

Fig 17 Variation Of Downforce with Thickness

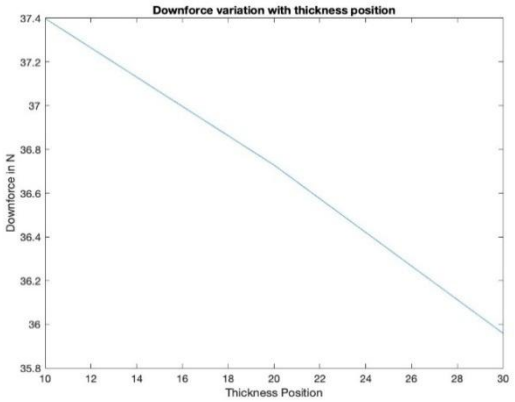

Fig 18 Variation Of Downforce with Thickness Position

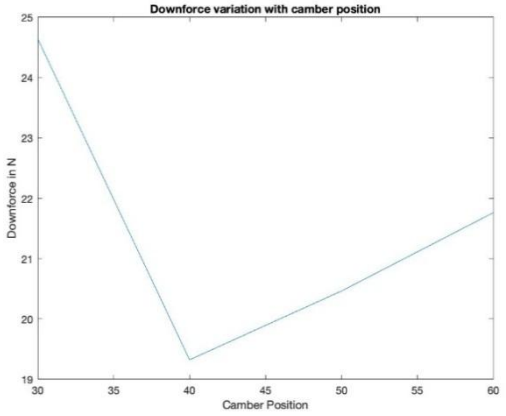

Fig 19 Variation Of Downforce with Camber Position

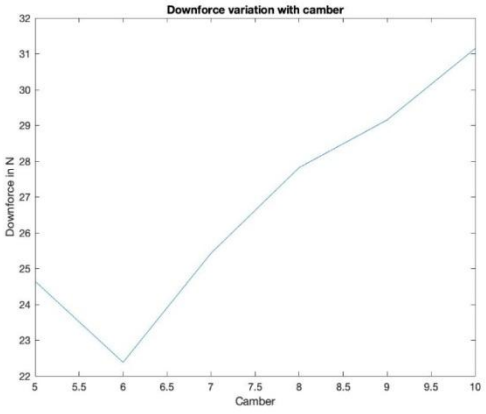

Fig 20 Variation Of Downforce with Comber Position

III. MANUFACTURING OBJECTIVE & RESULTS

The approach is to design a wing with increased stiffness and smooth surface finish emphasizing on the leading edge of the wing for enhanced aerodynamic properties. There are two manufacturing methods, a two-part, MDF mould which is easy to use and provides consistent results. However, obtaining optimum surface finish on the leading edge was proving to be difficult using the aforementioned method. The wing manufactured using a two-part MDF mould with a carbon fiber spar is taken as a benchmark for desired values of deflection corresponding to peak downforce and drag. The second method for wing manufacturing is using extruded polystyrene foam as a mould, which acts as a core for the wing. The motive for choosing this is the fact that this method helps us achieve a tailor-made finish on the leading edge, and also provides uniform stiffness throughout the cross-section of the wing, with better load transfer. This is demonstrated by performing a three-point bend test on a test laminate, where a 250N load is applied on the laminate and a deflection of less than 2.5 mm is observed, fulfilling the criteria mentioned in the FSAE rulebook for Formula Student Germany 2019.The mounting points and mounting system were also designed keeping the presence of foam as core in mind. Opting to use a material which solved two purposes at once, helped us reduce the costs greatly and also cut down on overall manufacturing time.

Structural simulation

For the structural simulation, ANSYS was used as the software of choice. The modules ACP pre, mathematical model and static structural were used for structural analysis of the front wing as depicted in figure 17. A fine mesh, with a relevance of 75 was chosen for accurate results, and the forces taken into consideration were 450N of downforce and 155N of drag, calculated at a speed of 120 kmph.

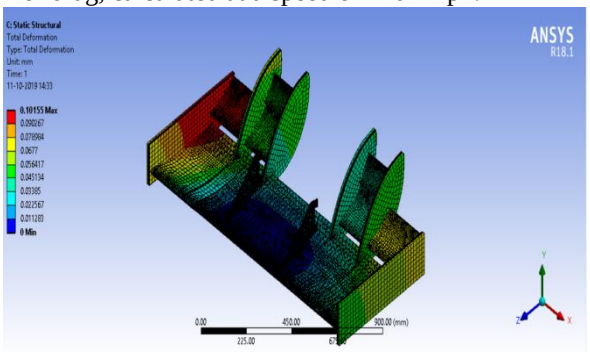

Fig. 17: Deformation obtained by finite element analysis

The deflection values obtained were a maximum of 0.1 mm, which were in accordance with the guidelines stated in the FSAE rulebook, which permits a maximum deflection of 2.5mm for a force of 250N applied on any 15X15 cm^2 cross-section of an aerodynamic device.

a. Material Selection

Mold:

The mould material was decided to be extruded polystyrene foam. This would provide a better surface finish on the leading edge of the wing, where it is of utmost importance. The mould also acts0 as a core for the wing, providing uniform stress distribution and load transfer.

Fiber :

The fiber of choice is carbon fiber. Contrasting it with glass fiber, it provides better mechanical properties of tensile and shear strength for lesser number of the layers. Also, mounting points on a carbon fiber laminate are more efficient than on a glass fiber laminate, due to the tendency of holes to get sheared over a short period of time in case of glass fiber. Comparing our choice to aramid fiber, the part would be of lighter weight if manufactured using carbon fiber, hence making it more efficient and driver-friendly.

Fig. 18: Shapes of carbon fiber layers prepared for lamination

Twill weave, 240 gsm dry carbon mat suitable for a wet layup process is used as can be seen in the setup shown in figure 18. Wet layup enables better monitoring of the leading edge during manufacturing to ensure a superior surface finish.

Resin :

Being aware of the fact that thermoplastics exhibit high viscosity and poor bonding, coupled by the fact that thermosetting plastics are easier to process, the natural choice was to go for a thermosetting polymer. Taking into consideration the availability, curing time and properties imparted to the laminate, epoxy (Atul L-12) was chosen.

b. Stack-up decision

To decide the ideal stack-up for a wing, extensive simulations were carried out on ANSYS for deflection upon application of load. Various different orientations of fabric were simulated, with different number of layers. The best possible result was obtained 2 layers of fiber followed by the foam core and two layers of fiber on the other side. A reserve factor of 2.6 was obtained for top values of downforce and drag, which was considered to be more than sufficient. Stackup of [CF2] two layers of carbon fibre was chosen.

IV. PROCESS REVIEW FOR MANUFACTURING

a. Mold manufacturing

The consumable foam core shown in figure 19 will also act as the male mold during the layup was manufactured by CNC machining of the foam in the required shape of the aerofoil. A wooden 3-axis spindle machine is used.

Fig. 19: Foam mold machined using 3 axis CNC machine

b. Mold surface preparation

After proper machining of the mold, getting the required surface finish is very important as it reflects on the final finish of the laminate. Therefore, the outer surfaces of the mold were sanded progressively using finer grades of Sandpapers to minimize the surface roughness as much as possible.

c. Prepare reinforcement:

Since covering the entire surface area in one layup was not the best option considering the factors that hand layup was used and the goal was to improve the leading edge, the layup was divided into two parts, first the layup will cover the complete lower surface and will spread up to twenty percent of the upper surface, the second layup will cover the remaining upper surface. The stencils were made accordingly and fibers in the shapes were cut out off in the decided number of layers.

d. Prepare Matrix:

The optimum reinforcement to matrix ratio was conceived by doing several iterations which involved mixing of range of different ratios. The final ratio was obtained based on the balance of properties of the required laminate weighing brittleness and stiffness as the parameters. The resin was decided and suitable hardener was acquired. Hence the matrix was prepared by mixing the predetermined ratio of resin with hardener for the application as depicted in figure 20.

Fig. 20: Application of the liquid resin prepared

e. Apply Layers:

The layers of fabric are laid one after another starting initially with a layer of liquid resin on the mold and applying resin after every layer of fabric. They are positioned manually in a single sided male mould with the application of liquid resin over the mold and the reinforcement placed on top, visible in figure 21. After applying the last of resin on the fabric a release film (a perforated sheet of plastic) is laid which has a pre-applied releasing agent on it and is supposed to help with removal of breather cloth (a non-woven polyester fabric) during the demoulding. Last a layer of breather is laid on the complete layup to allow the airflow when the pressure is applied and is also presumed to soak all the excess resin.

Fig. 21: Performing layup in the decided stackup

f. Vacuum bag:

The complete layup was put inside a vacuum bag and sealed before connecting it to a vacuum pump in order to mechanically pressurize the laminate as depicted in figure 22. This process removes the trapped air between the layers, and also consolidates the layer to enable efficient force transmissions. Vacuum bagging applies uniform pressure on the laminate inside thus prevents the shifting of fiber orientation. The reinforcement to matrix ratio in the composite was optimized in order to obtain maximum strength. Reaching an optimum ratio is necessary as lesser reinforcement will make the laminate brittle and lesser matrix will make it weak on the dry spots. A maximized ratio is obtained by saturating the reinforcement that is laminating without any excess resin.

Fig. 22: Vacuum bagging process

g. Curing and demoulding:

The curing is done at a room temperature and left out according to time as per the cure life of the matrix. After curing is done the vacuum bag is opened and the breather cloth is released from the release film.

h. Rib bonding:

Ribs designed in the shape of respective aerofoil were used to solve the problem of attaching the wing element to the end plates on both sides. The balsa ribs were bonded to the wing sides where the foam is visible using epoxy resin. Location for the holes were predetermined and holes were dug in the foam where the bolt heads will go while they were inserted in the foam through the balsa ribs inside out while bonding. Stencils were Laser cut in an aerofoil profile to assist the rib cut outs from balsa sheets and to locate the holes from the bolts will go. The balsa ribs with assembly bolts attached is shown in figure 23.

Fig. 23: Balsa ribs ready for bonding

i. Surface finish:

The exposed surfaced over the laminate was further improved in surface finish by using incremental Sandpaper grades to obtain aerodynamically optimized surfaces. Finished and assembled front wing can be seen in figure 24.

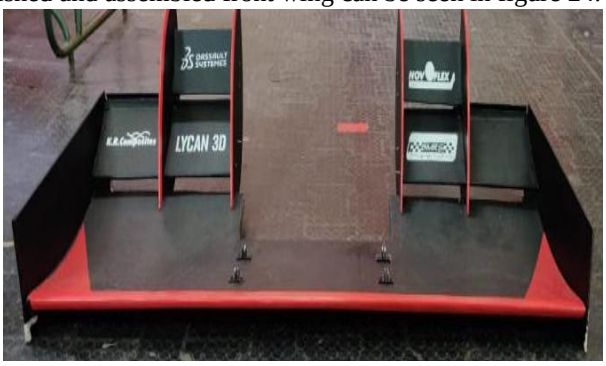

Fig. 24: Final wing structure

j. Testing and Validation:

A three-point bend test was performed on a test laminate, a setup for which is depicted in figure 25. In the experimental test a 250N load is applied according to the fulfilling the criteria mentioned in the FSAE rulebook for Formula Student Germany 2019. on the laminate and a deflection of less than 2.5 mm is observed. The modulus of the test sample was obtained to be 6319.8 MPa thus satisfying the strength requirements.

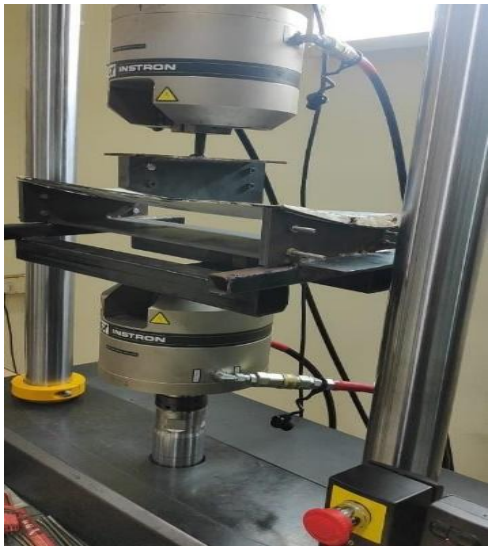

Fig. 25: 3-point bend test setup

V. CONCLUSION

The study concluded that out of the parameters that are , camber position, thickness, camber and thickness position. The most significant parameter was the camber. The downforce increased by 11N. The drag mostly remained the same with an increase of only 0.3N. The footplates played an important role in increase the aspect ratio of the vehicle.

Manufacturing method is chosen from the several manufacturing processes that can be used in the production of high-performance aerodynamic devices. The process is optimized by improving and simplifying the method which aids in better aerodynamics and also ease of assembly. The optimization in the final product is done by reducing the total weight from 4.7kgs to 3.9kgs as well as increasing stiffness and integrity which was determined through experimental data.

The manufacturability of the carbon fiber components was also increased and the cost of tooling was cut down since male molds with machining cost close to Rs. 4000 require lesser tooling as compared to the conventional female molds which cost around Rs. 25000. As the requirements evolve a polished surface for increased aerodynamic outcome is also provided. Thus, a Composite Structure is strongly recommended due to the significant cost and weight savings and increase in both strength and stiffness.

REFERENCES

1. Manufacturing Aspects of Advanced Polymer Composites for Automotive Applications Springer Science+Business Media B.V. 2012 : Klaus Friedrich & Abdulhakim A. Almajid
2. Composite materials for aerospace applications Aeronautical Development Aeronautical Development Agency, Vimanapura PO, Bangalore 560017, India . Bull. Mater. Sci., Vol. 22, No. 3, May 1999, pp. 657-664. © Indian Academy of Sciences.: P D MANGALGIRI
3. Monolithic composite wing manufacturing process - US Patent 6,190,484, 2001: K Appa
4. Ultralight composite wing structure - US Patent 4,538,780, 1985 - Google Patents: RD Roe
5. Fabrication and Structural Equivalency Analysis of CFRP Nomex Core Sandwiched Panels for FSAE Race Car Chassis University of New South Wales at the Australian Defence Force Academy: Muhammad Yaqoob
6. Formula SAE Vehicle Aerodynamics - The UNSW Canberra at ADFA the UNSW Canberra at ADFA Journal of Undergraduate Engineering Research, 2008 - ojs.unsw.adfa.edu.au: M James
7. Control of Low-Speed Airfoil Aerodynamics-Gad-el-Hak, M., 1990,AIAA J., 28[9], pp. 1537–1552
8. Separation Control: Review- Gad-el-Hak, M., and Bushnell, D. M., 1991, ASME J. Fluids Eng., 113, pp. 5–30,
9. Aerodynamics of a Single Element Wing in Ground Effect, Zerihan, J., and Zhang, X., 2000, J. Aircr., 37[6[, pp. 1058–1064.
10. Off-Surface Aerodynamic Measurements of a Wing in Ground Effect, Zhang, X., and Zerihan, J., 2003, " J. Aircr., 40[4[, pp. 716–725.
11. Aerodynamics of a Double-Element Wing in Ground Effect Zhang, X., and Zerihan, J., 2003,AIAA J., 41[6], pp. 1007–1016.
12. Edge Vortices of a Double-Element Wing in Ground Effect, Zhang, X., and Zerihan, J., 2004 "J. Aircr., 41[5], pp. 1127–1137